Egyptian Geophysical Society
EGS Journal, Vol. 9, No. 1, 51-59 (2011)

AN INTEGRATED APPROACH TO INDICATE EDGE MAPPING AND AEROMAGNITIC DEPTH SOLUTIONS

S.M.M. Hanafy
Nuclear Materials Authority

رؤية متكاملة تؤدى إلى تحديد الحواف وتقدير الأعماق لبيانات المغناطيسية الجوية

الخلاصة: تم تطبيق عدد من الطرق مثل التحليل الطيفى وطريقة فيرنر و طريقة اويلر بالإضافة إلى طريقة النمذجة ثنائية الأبعاد على بيانات المغناطيسية الجوية فى تحديد الحواف وتقدير الأعماق لمنطقة تقع جنوب الصحراء الشرقية. تم استخدام الخريطة المغناطيسية لمنطقة وادى خريط والتى تقع بين خطى عرض`20 º24 – `45 º24 شمالاً وخطى طول`20 º33 - `40 º33 شرقاً كمثال لتطبيق الرؤية المتكاملة حيث تم وضع البيانات المغناطيسية فى صور شبكية و تم فصل الشاذات المغناطيسية باستخدام طريقة التحليل الطيفى بالإضافة إلى تفسير مكان المصدر وعمقه بواسطة مفكوك أويلر المتجانس حيث تم استخدام هذه النتائج فى رسم خريطة تركيبية لصخور القاعدة مع تطبيق طريقة فيرنر "باستخدام نظرية النافذة المتحركة" على خط مغناطيسى فى الاتجاه الشمالى الشرقى–الجنوبى الغربى، وتصدير هذه الحلول إلى برنامج النمذجة ثنائية الأبعاد، وذلك لعمل مقارنة مباشرة بين حلول تقدير الأعماق مع السطح الهندسى لصخور القاعدة.

ABSTRACT: *Edge and depth analysis using spectral analysis, Euler deconvolution, Werner deconvolution and inverse modeling techniques has been performed on aeromagnetic data. Wadi Kharit magnetic map was used as an example towards the desired integrated approach. The area is located in the South Eastern Desert between latitudes 24 °20` and 24° 45`N, and longitudes 32° 40` and 33° 20` E. Magnetic survey data in a grid form were generated, isolation of magnetic anomalies using spectral analysis was conducted, as well as the interpretations for source position and depths by deconvolution using Euler's homogeneity relation were performed. Results obtained from spectral analysis and Euler deconvolution were used to construct a basement tectonic map. The automatic Werner deconvolution method (using the moving window concept) was applied to the NE-SW magnetic profile. The resulting solutions have been selected to be exported to the GM-SYS model. A direct comparison could be made between the magnetic depth solutions and geometric surface of the basement using simultaneous 2D modeling of magnetic data along the profile.*

INTRODUCTION

The present work addresses the problems encountered in magnetic depth estimation and the problem of edge effect in the interpretation of magnetic data. In addition comprises a comparative study in which we discuss and critically assess base definitions and assumptions associated with each method.The main tectonic feature recognized in this area is a huge NW-SE sedimentary basin, underlain by Precambrian basement rocks, which outcrops in different localities of the study area (Fig. 2).

The main wadi, in this area, is wadi Kharit pursuing at first a northwesterly course where the valley widens into a broad plain bounded by an undulating sandstone desert on the west side and by sandstone hills on the eastside.

The reduced to pole magnetic profile was extracted in the NE-SW direction at a right angle to the basin's major axis. Wells which were drilled in the area at the eastern end of the profile were used to support the depth calculations.

SOFTWARE

Edge mapping and depths to basement were calculated using Oasis montage data processing and analysis system (Geosoft, 2002). The spectral analysis using MAGMAP 2D-FFT system, supports common Fourier domain filters to gridded data.

Fig. (1) Location map of the study area.

The standard Euler 3D deconvolution is automatic location and depth determination software for gridded potential field data. Werner deconvolution operates under the "Pdepth" menu. Window Shift Increment sets the distance through which the Werner operator is moved along the profile between calculations (the moving window concept). 2-D simultaneous magnetic modeling was carried out using GM-SYS software program (Geosoft, 1999).

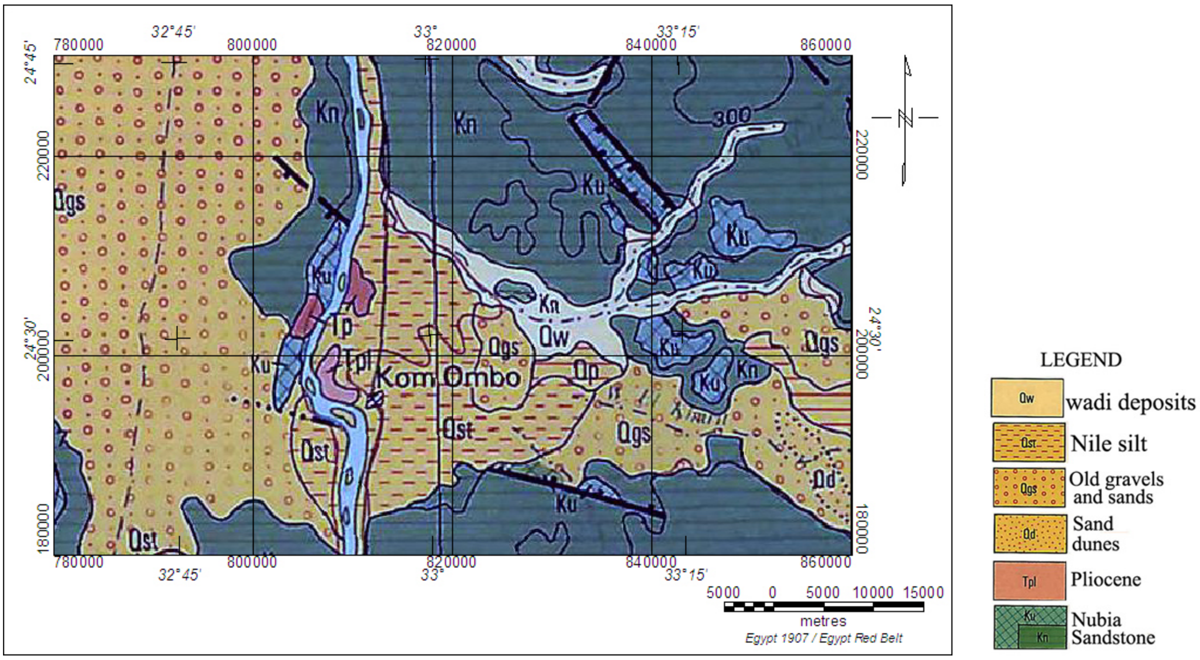

Fig. (2): Geological map of wadi kharit area, Eastern Desert, Egypt. (EGSMA, 1979)

The total magnetic data were iteratively utilized on the geological model, till a good fit is reached between the observed and calculated profiles.

Processing of The Aeromagnetic Survey Data

Reduction to the north magnetic pole was performed at the first stage of processing. The azimuthally averaged logarithmic power spectrum was computed. The spectral slope (Geosoft, 2002) technique was applied to each. Isolation of anomalies was achieved using Butterworth regional /residual separation filters conducted for the RTP map into deep regional and shallow residual components. Euler deconvolution (Ried, et al, 1990) comrises both a boundary finder and a depth estimator. Some indications of the source type may be gained by varying the structural index for any particular feature. The Werner deconvolution (Ku and Sharp, 1983) technique discussed in this work interprets profile data. Estimated depths may also provide a good starting point for a genuine structural interpretation using interactive modeling.

An integrated approach

Xiong Li (2003) recommends an integrated approach to deriving an accurate depth solution. This approach involves the following essential aspects:

1. Selection of the proper or optimal methods.
2. Applying more than one reasonable method to the same data set.
3. Suggesting possible ways to overcome or avoid the three difficulties (the moving window, the source geometry and the derivative calculation)
4. Carefully picking the geologically most plausible solutions.
5. Examination of the position of the significant anomaly on the image/map of gridded results. The profile should cross the 2D body at a right angle to the strike and near the center.
6. Comparison of the solutions on adjacent lines.
7. Using all geological, geophysical data, and well controls that are available.
8. Using a good 3D visualization tool to display depth solutions.

This work explores assumptions behind different methods and demonstrates examples through which better solutions can be obtained, only when a proper method is selected according to the data quality and source geometry assumption. It is possible to expand this approach to include the edge mapping.

RESULTS AND DISCUSSION

Isolation of anomalies using the Butterworth regional/residual separation filters are conducted on the RTP map (Fig. 3). The azimuthally averaged logarithmic power spectrum was computed (Fig. 4). The log spectrum shows two parts, deep regional (Frequency= 0.0 to 0.05) and shallow residual (Frequency= 0.05 to 0.2). The interactive spectrum technique was applied to each. The residual map Fig. (5) exhibits the local anomalies, which reflect the near-surface structures, while the regional map Fig. (6) reflects the broad anomalies related to the deep-seated changes in the structures of the basement rocks.

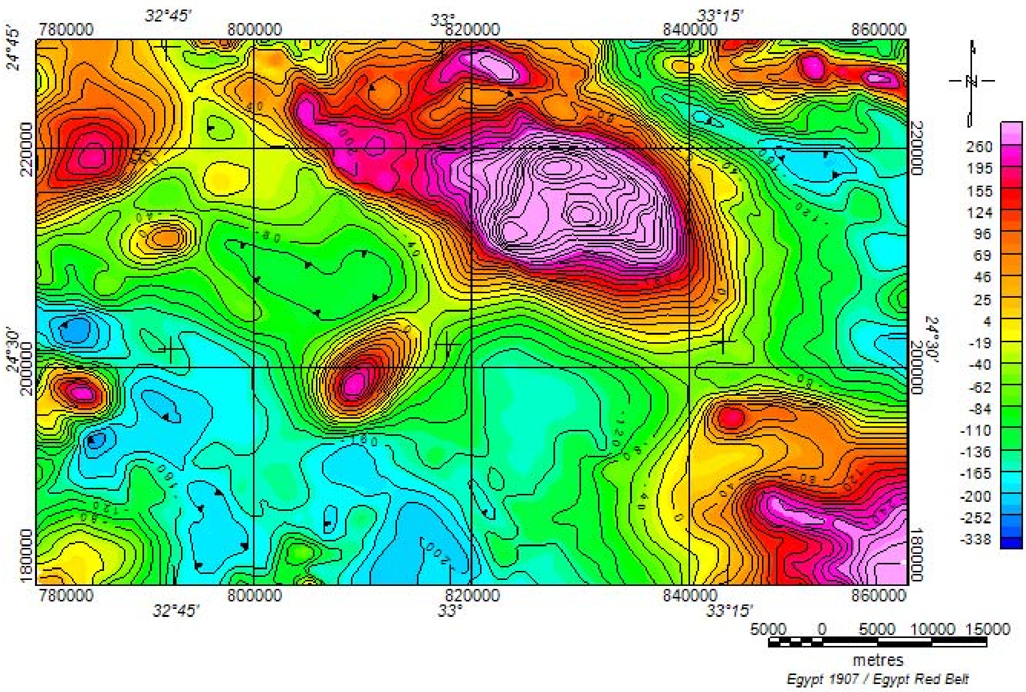

Fig. (3): Total intensity magnetic map, reduced to the North magnetic pole, Wadi Kharit area, Eastern Desert, Egypt. (Aeroservice, 1984)

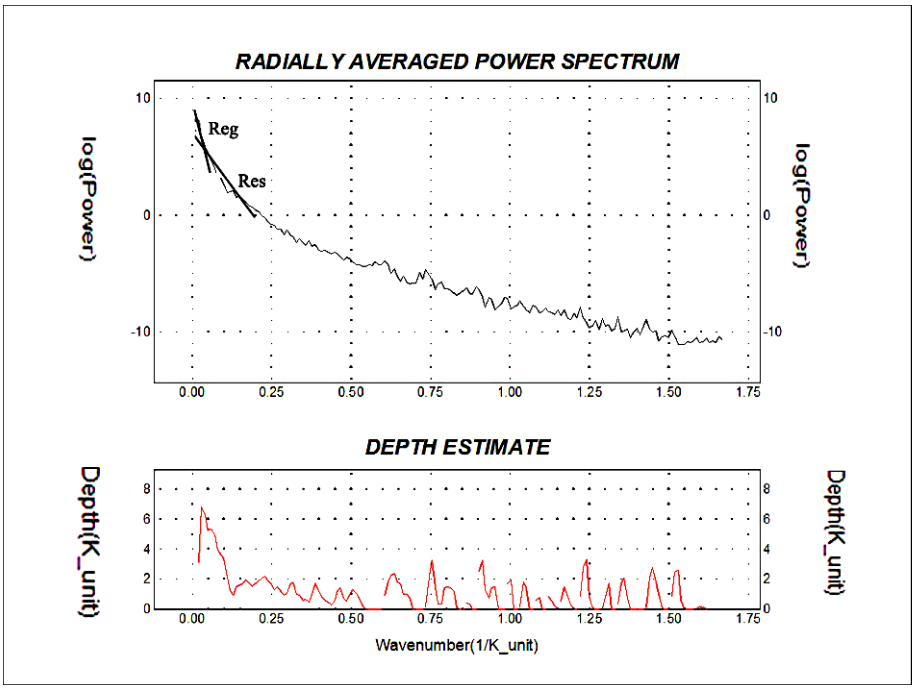

Fig. (4): A typical interpretation of the energy (power) spectrum with the average depths to the deep and shallow surface sources.

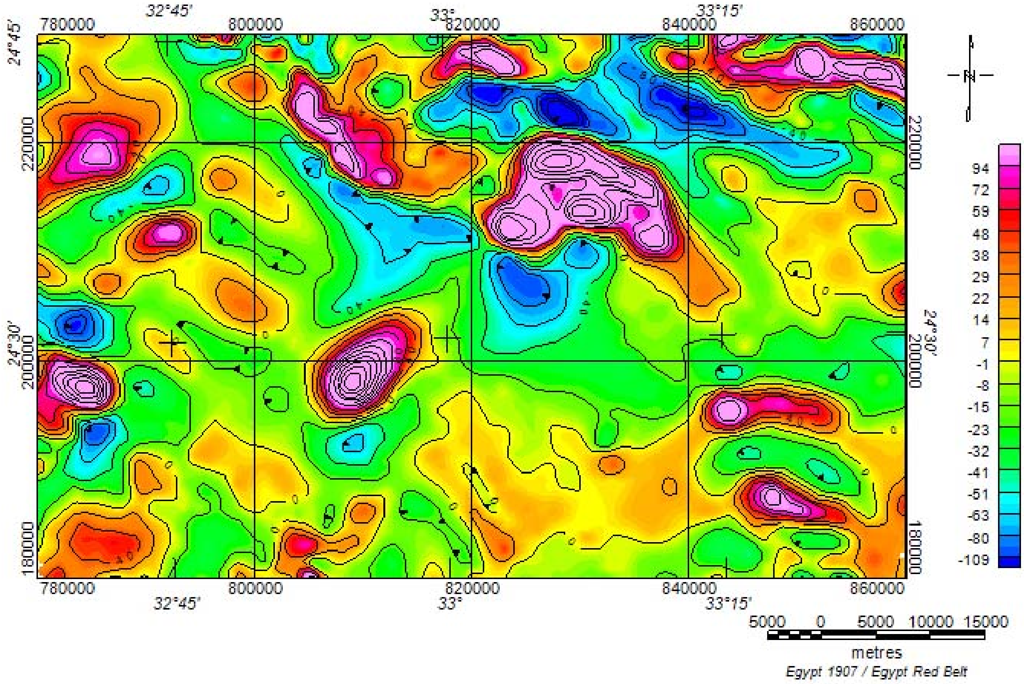

Fig. (5): Residual magnetic component map (Butterworth filter), Wadi Kharit area, Eastern Desert, Egypt.

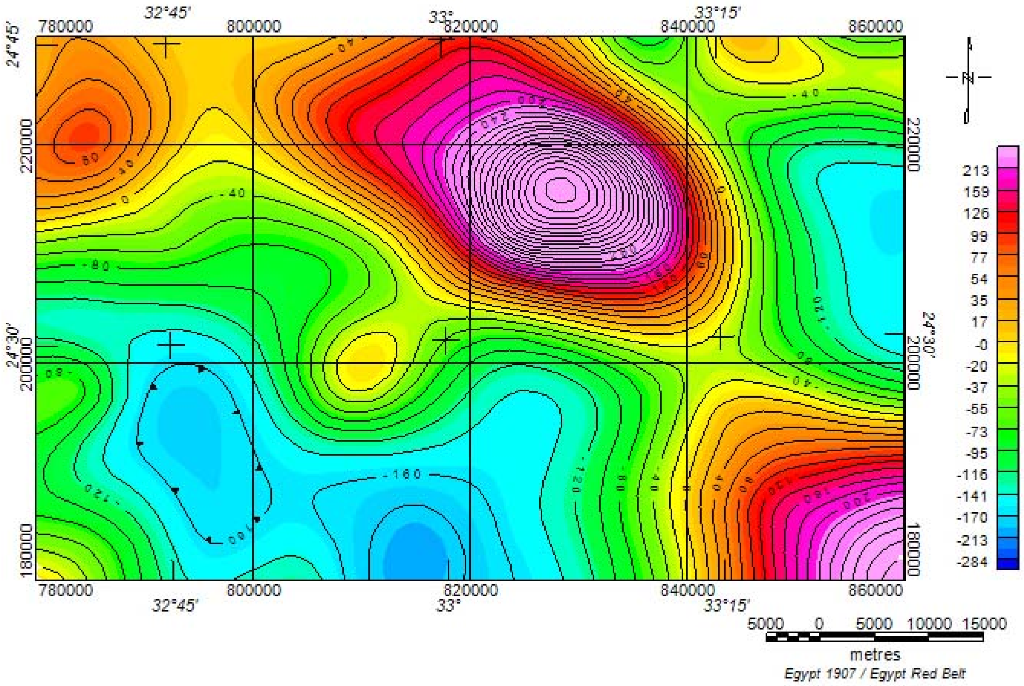

Fig. (6): Regional magnetic component map (Butterworth filter), Wadi Kharit area, Eastern Desert, Egypt.

The Butterworth filter is excellent for applying straight forward high pass and low pass filters to data because it can easily control the degree of filter roll-off while leaving the central wave number fixed. If ringing is observed, the degree can be reduced until acceptable.

The Euler 3D Deconvolution system is designed to work on processed gridded data. The deconvolution process is to compute a set of x, y, and z derivative grids that are required for the Euler source inversion calculation. The search window size determines the area (in grid cells) used to calculate the Euler solutions. In the present example, the anomalies of interest are mostly 3-6 km in width therefore a good estimate for the search window size is about 6 km. The grid cell size is 320 m, this corresponds to about 20 grid cells. The Euler deconvolution maps (Figures 7-9) present the derived source positions as circles at their plan positions with depth proportional to diameter. They show roughly the same trends at all three structural indices, but with different degrees of clustering and depths. The correct index for any given feature was chosen as that which gave the tightest clustering, when this could be distinguished. The linear contact features trending NW faults (forming two uplifted platforms in the north and south of the study area and leaving the central part as large basinal area covered with the sediments) show the best clustering using index 0.0 (given by the symbol size on Figure 7). The thick step feature is seen using index 0.5 (Fig. 8). Sill and dyke is likely to be a subsidiary fault with vertical displacement suggested by index 1.0 (Fig. 9). Structures such as contacts are surrounded by a cloud of poorly defined solutions, which obscure the better solutions.

In practice, some undesired, scattered solutions are accepted for the sake of defining as many structures as possible. It is likely to be a feature of little depth extent. A similar Euler approach was applied to all the features shown, together with reference to the contour maps (Figures 3, 5 and 6), to arrive at a subsurface integration. The results were classified by comparison with the independent information described above and the interpretation is shown in Figure 10.

The automatic depth estimate can often generate a quick (much quicker than magnetic inversion) interpretation of magnetic profile data. So, it is useful to recommend an integrated approach for deriving an accurate depth solution.

Profile (A-A’) shown in Fig. (3) was extracted from the RTP magnetic map, perpendicular to the basin’s major axis. Figure 11 shows a total magnetic field profile with the calculated horizontal derivative (upper panel) and its final depth solution produced by Werner deconvolution method (lower panel). It indicates several groups of good solutions (diamond) derived from the total field profile designated as "Dike" solutions, and several groups of solutions (rectangle) derived from the horizontal gradient are designated "Contact" solutions. All “dike” solutions should line up with peaks in the magnetic profile and all “contact” solutions should line up with peaks in the horizontal gradient profile. Dike solutions and contact solutions are clustered in separate runs.

These are very useful to locate the subsurface magnetic sources, which reflect the geologic structures. Because the deep basement is of interest, the solutions resulted from Werner deconvolution method have been selected to be exported to GM-SYS model. A direct comparison can be made between the magnetic depth solutions and geometric surface of the basement, using simultaneous 2D modeling of magnetic data along the profile.

The total magnetic data were iteratively utilized for the geological model, until a good fit is reached between the observed and calculated profiles. Figure 12 shows the modeled total magnetic profile shown in the upper panel. The geometric surface of the basement with the final depth solutions derived by the automatic Werner deconvolution method together with the four wells, which were drilled in the area (Komobo-1, Komobo-2, Komobo-3 and Elbaraka-1), are shown in the lower panel. They did give useful minimum depth estimates in areas of deep basement. The calculated depth values derived from the Werner deconvolution method are in agreement with the depth information obtained from the modeling process and drill holes. The final depth solutions derived by the integrated approach. are shown in Table 1.

CONCLUSIONS

This work explores assumptions behind different methods and demonstrates examples through which better solutions can be obtained. Edge and depth analysis using these techniques has been performed on aeromagnetic data on a study area located South Eastern Desert of Egypt as a sample area for demonstration.

Four techniques were used to estimate depths to magnetic basement, the structure and to define geologic description. The Butterworth filter is excellent for applying straightforward high pass and low pass filters. Euler deconvolution is both a boundary finder and a depth estimator. Some indications of the source type may be gained by varying the structural index for any particular feature. However, users need to make a right decision about the structural index. Results obtained were used to construct a basement tectonic map. The Werner deconvolution technique interprets a profile data and produces better depth estimate. Estimated depths may also provide a good starting point for a genuine structural interpretation using interactive modeling. The integrated approach recommended in this work will help derive final and accurate solution.

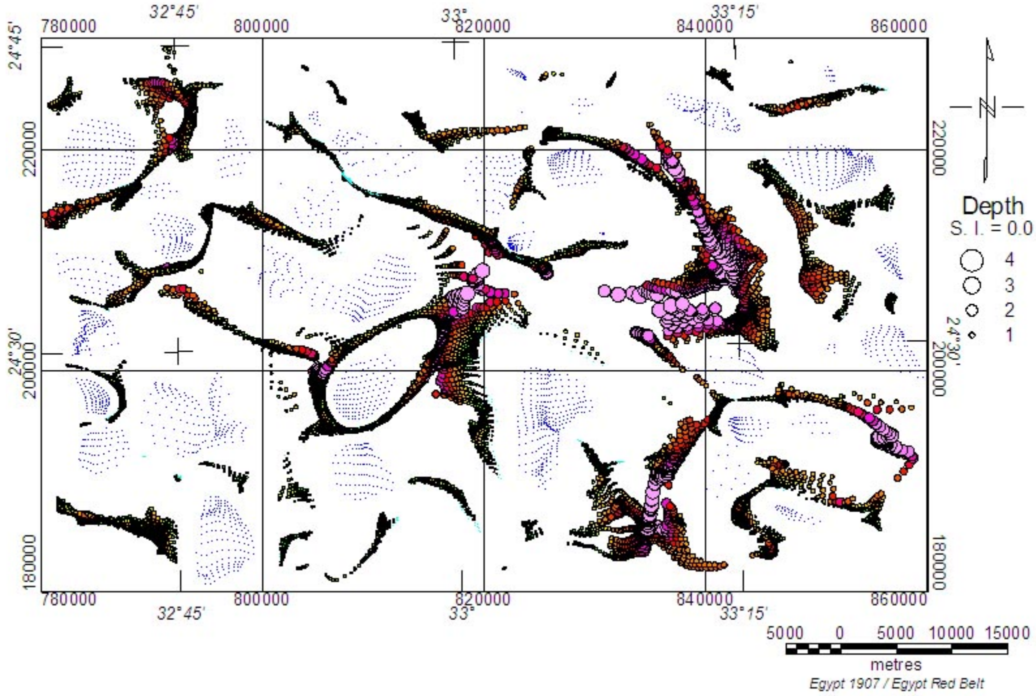

Fig. (7): Euler Deconvolution magnetic map (S. I. =0.0), Wadi Kharit area, Eastern Desert, Egypt.

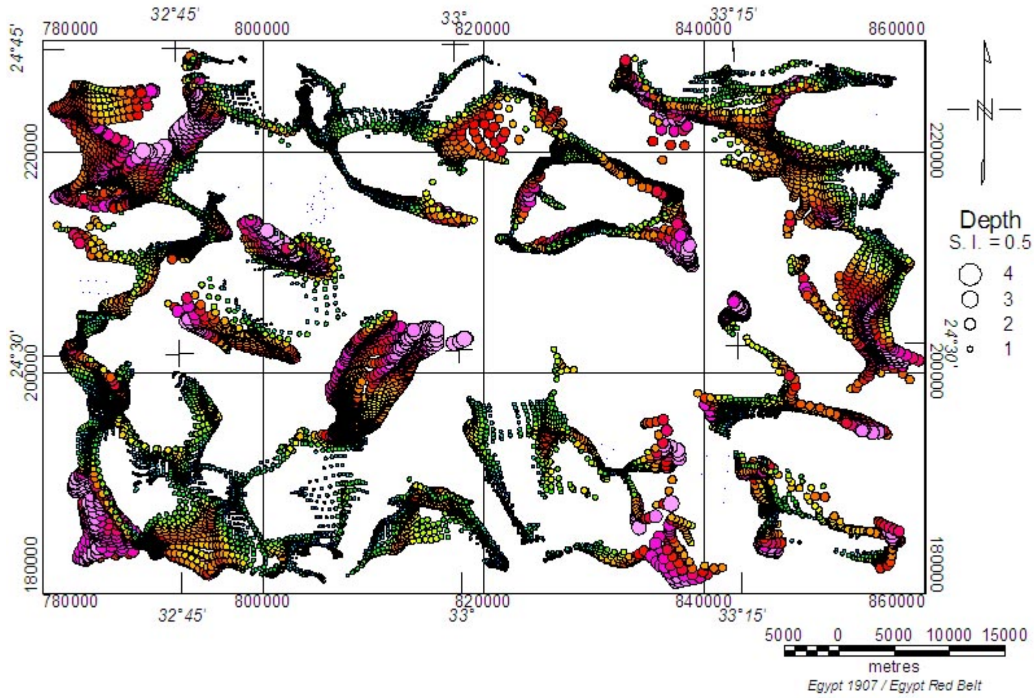

Fig. (8): Euler Deconvolution magnetic map (S. I. =0.5), Wadi Kharit area, Eastern Desert, Egypt.

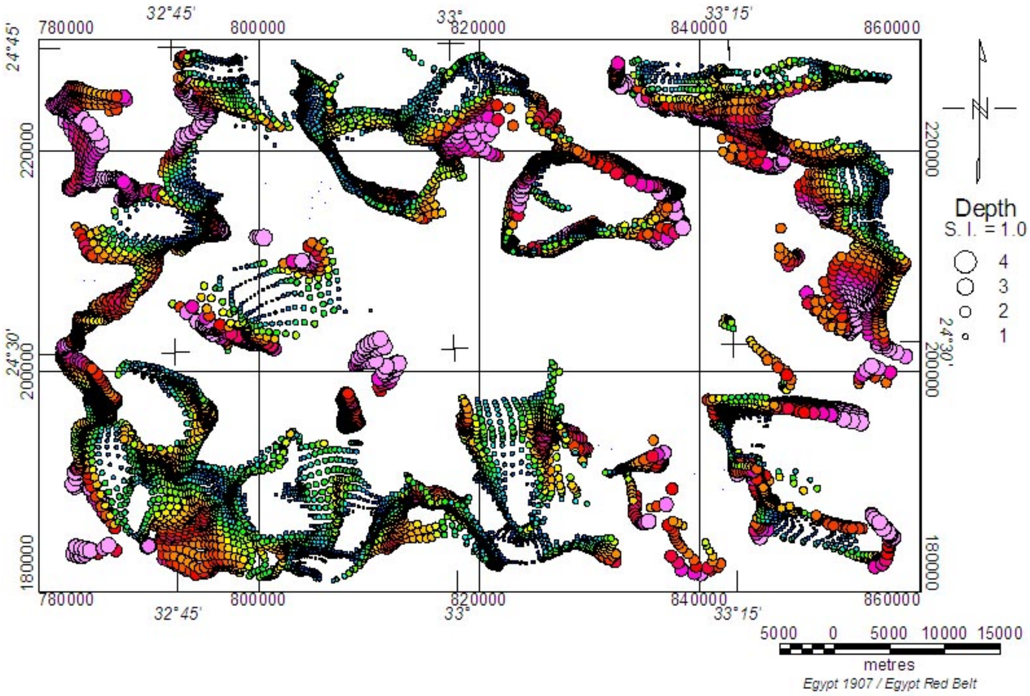

Fig. (9): Euler Deconvolution magnetic map (S. I. =1.0),
Wadi Kharit area, Eastern Desert, Egypt.

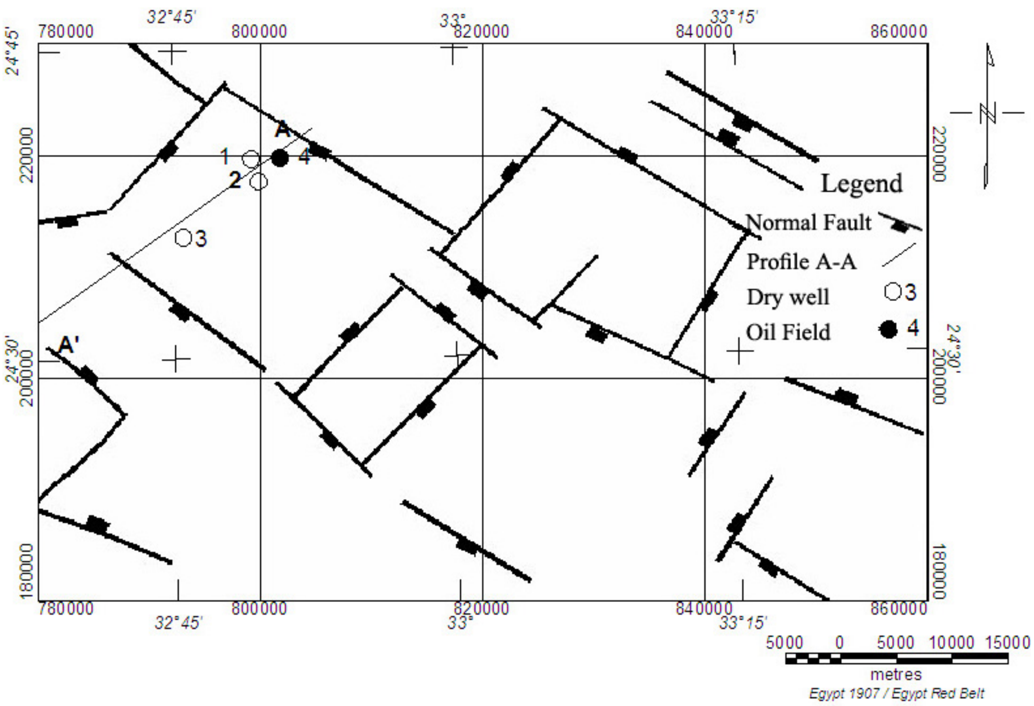

Fig. (10): The interpreted basement tectonic map,
Wadi Kharit area, Eastern Desert, Egypt.

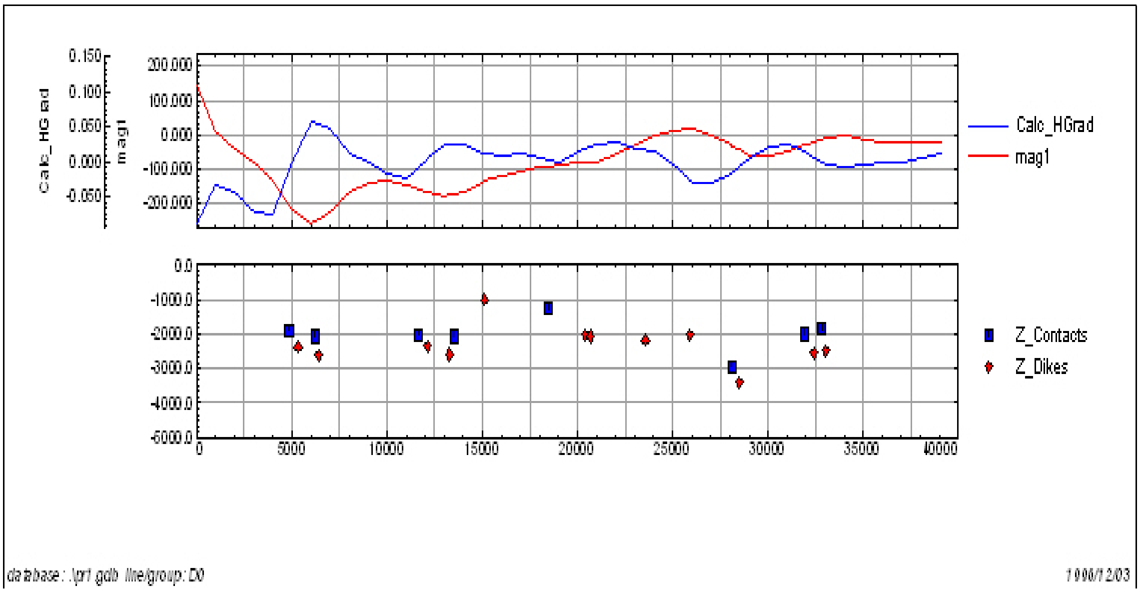

Fig. (11): A real data profile of total field magnetic data, with the calculated horizontal derivative of TM (upper panel), and the final depths estimated by the Werner deconvolution method (lower panel).

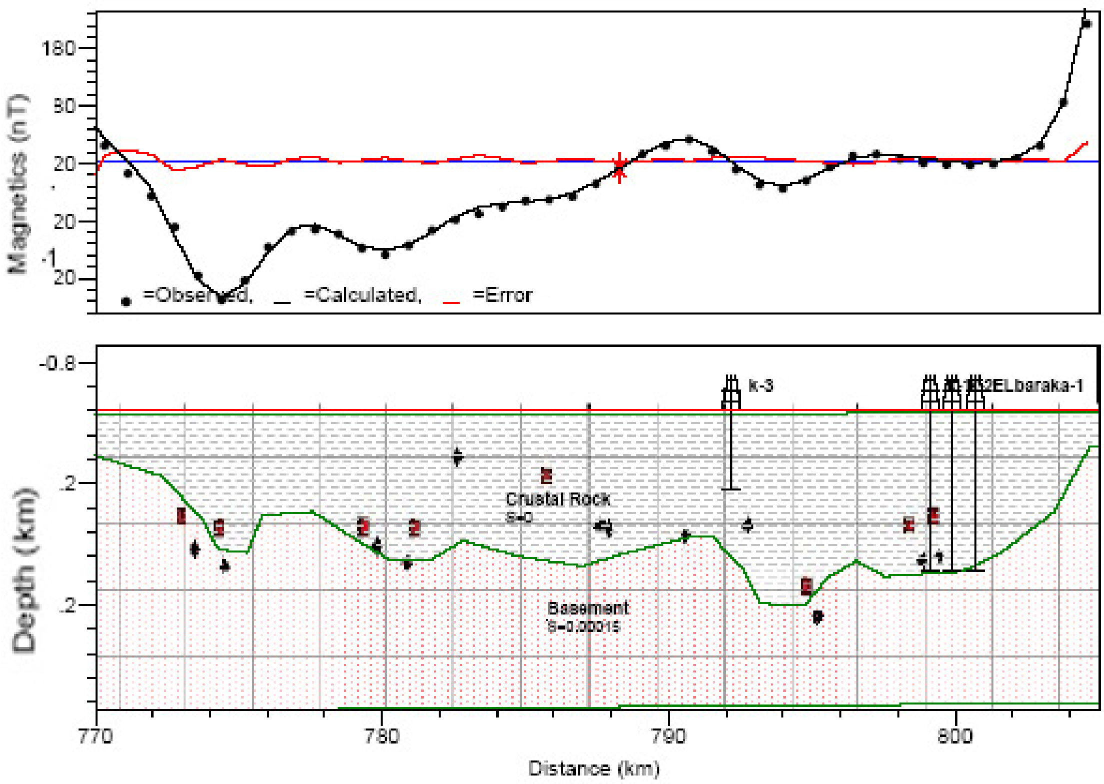

Fig. (12): The two-dimensional modeled total magnetic field profile, Wadi Kharit area, Eastern Desert, Egypt.

Table (1): Estimated Depth (in Feet) From Werner Deconvolution and Modeling Process Compared With Data From Drilled Holes.

Well Name	**Drilled Holes**	**Werner Deconvolution**		**Modeling Process**	
	Depth (Feet)	**Depth**	**% err**	**Depth**	**%err**
Komobo-1	8641 (oil shows)	8230	4.11	8671	0.30
Komobo-2	8632 (oil shows)	8044	5.88	8671	0.39
Komobo-3	4205 (dry well) **	6094	**	7486	**
Elbaraka-1	8740 (oil field)	8044	6.96	8415	3.25

*** Drilling stopped at this level*

REFERENCES

Aeroservice, 1984, Final operational report of airborne magnetic and radiation survey in the Eastern Desert, Egypt. Aeroservice, Houston, Texas, April 1984, six volumes, 1-127.

Egyptian Geological Survey and Mining Authority, (1979), Geological map of Aswan, Egypt. NG36, scale 1:100000. Geol. Surv., Egypt., Cairo. 1 map.

Geosoft Inc., 1999, GM-SYS modeling of potential field data. Geosoft Inc., Toronto, Canada.

Geosoft Inc., 2002, Oasis montage data processing and analysis system. Geosoft Inc., Toronto, Canada.

Ku, C. C., and Sharp, J. A., 1983, Werner method for automated magnetic interpretation and its refinement using Marquardt inverse modeling: Geophysics, 48, 754-774.

Ried, A. B., Allsop, J. M., Granser, H,, Millet, A. J., Somerton, I. W., 1990, Magnetic interpretation in the three dimensions using Euler Deconvolution, Geophysics. Vol. 55, pp. 80-91.

Xiong Li., 2003, On the use of different methods for estimating magnetic depth, Fugro-LCT Inc., Houston, Texas.